Contents lists available at ScienceDirect

Waste Management

journal homepage: www.elsevier.com/locate/wasman

Revealing hydrodynamics and energy efficiency of mixing for high-solid anaerobic digestion of waste activated sludge

Min-Hua Cui [a,b,1], Zhi-Yong Zheng [a,b,1], Meng Yang [a], Thangavel Sangeetha [c], Yan Zhang [a,b], Hong-Bo Liu [a,b], Bo Fu [a,b], He Liu [a,b,*], Chong-Jun Chen [b]

[a] Jiangsu Key Laboratory of Anaerobic Biotechnology, School of Environmental and Civil Engineering, Jiangnan University, Wuxi 214122, PR China
[b] Jiangsu Collaborative Innovation Center of Technology and Material of Water Treatment, Suzhou 215011, PR China
[c] Department of Energy and Refrigerating Air-Conditioning Engineering and Research Center of Energy Conservation for New Generation of Residential, Commercial, and Industrial Sectors, National Taipei University of Technology, Taipei 10608, Taiwan

ARTICLE INFO

ABSTRACT

Anaerobic digestion is a feasible and promising technique to deal with emerging waste activated sludge issues. In this work, the hydrodynamics and digestion performance of horizontal anaerobic systems equipped with double-bladed impeller and ribbon impeller were investigated. Simulation using computational fluid dynamics technique visually showcased the favorable mixing status implementing ribbon impeller. The mixing modes were considered as the major motivation for the difference of mixing efficiencies. Tracing experiment indicated that the minimum thorough mixing time with ribbon impeller was 20 min at a rotation speed of 50 rpm, whereas it was 360 min for the double-bladed impeller under similar conditions. The superior mixing performance of ribbon impeller resulted in better anaerobic digestion and energy efficiency outputs. The digester employing ribbon impeller obtained an ultimate biogas yield of 340.38 ± 15.91 mL/g VS (corresponding methane yield of 210.34 ± 7.55 mL/g VS) and produced a surplus energy of 16.23 ± 0.76 $MJ/(m^3 \cdot d)$. This study thus ascertained that ribbon impeller was proficient for high-solid anaerobic digestion and it will prominently benefit future system designs.

© 2020 Elsevier Ltd. All rights reserved.

1. Introduction

In biological treatment technology, activated sludge process in particular, is widely applied to address wastewater issues due to its advantages like high efficiency, affordability, and easy operation (Liu et al., 2019a). The waste activated sludge (WAS) is one of the most concerned by-products during biological wastewater treatment. It is estimated that the annual WAS production will accomplish 60 million tons (based on 80% of moisture content) in China by the year 2020 (Wei et al., 2020). The anaerobic digestion is a recommended treatment method for WAS due to its cost-efficient and resource recovery capacities (Sadino-Riquelme et al., 2018). In terms of the practical application of anaerobic digestion, utilization of high-solid content (total solid > 10%) of WAS is a feasible strategy to minimize the reactor volume and the post-treatment of digestate (Pastor-Poquet et al., 2019a; Pastor-Poquet et al., 2019b).

The WAS with relatively low-solid content (total solid < 2.5%) can be deliberated as a Newtonian fluid and it had transitioned to a non-Newtonian fluid along with solid content increase (Wu, 2012). The rheology of non-Newtonian fluid was reported to have distinctly changed from Newtonian fluid, along with the variation of flow characteristic. It is well known that mixing process is indispensable in high-solid WAS anaerobic digestion which is used to obtain the homogeneous substrate, functional microbes, eliminate stratification, uniform distribution of heat and facilitate the transfer of gas (Singh et al., 2019). The mixing efficiency is a crucial factor to influence the performance of WAS anaerobic digestion as well as energy efficiency. The mixing energy consumption has been evaluated to account for up to half of the biogas plants that have implemented WAS digestion (Kowalczyk et al., 2013). Current practices in WAS digester designs are needed to be updated and there is an earnestness to exploit an alternative approach to anaerobic digestion energy output (Dapelo and Bridgeman, 2018).

Various categories of impellers have been tested in anaerobic digestion systems, including bladed impeller, ribbon impeller, anchor impeller, curtain-type impeller, etc. (Wu, 2012). Among

---

* Corresponding author at: Jiangsu Key Laboratory of Anaerobic Biotechnology, School of Environmental and Civil Engineering, Jiangnan University, Wuxi 214122, PR China.
E-mail address: liuhe@jiangnan.edu.cn (H. Liu).
[1] These authors contributed equally to this work.

them all, the bladed impeller is one of the most common used impeller type due to the simple construction. The mixing process in a digester with bladed impeller normally starts from the center of the reactor near the mixer shaft. The ribbon impeller provides larger stirring diameter and activates the mixing process from the periphery to the center of the digester. Whereas the effect of the different mixing modes between the bladed impeller and ribbon impeller on the WAS digestion remains unclear, especially in the horizontal anaerobic system. In addition to the impeller type, the mixing strategy is the pivotal concern for the optimization of mixing. The intermittent mixing was proved as an alternative strategy to continuous mixing or unmixing for high efficient biogas production and energy saving, and a mixing time of 2 min/h was optimized for almost entirely homogeneous of anaerobic digestion of food waste (Zhang et al., 2019). The turbine impeller with a blade angle of 30° and mixing time of 5 min consumed the least energy whereas produced the most CH$_4$ amounts associated with added total solid degradation (Mahmoodi-Eshkaftaki and Ebrahimi, 2019). However, the simultaneous evaluation of the influence of impeller type and mixing strategy on the WAS anaerobic digestion is still not clearly studied, and the reason for the differences in mixing efficiencies of various impellers requires to be elucidated.

It is significant to visually depict the mixing process with various impeller construction and mixing tactics. Owning to the rapid development and powerful functions of computational fluid dynamics (CFD) technology, the specific information could be inquired at an optional position of the desired flow field and the vivid flow pattern representation of the bioreactors at various conditions have been made detectable (Cui et al., 2020). CFD visualization of anaerobic digestion of WAS in vertical bioreactors was observed to be feasible (Wu, 2012), yet the energy efficiency associated with mixing performance requires imperative clarification.

In this work, two types of impellers, namely double-bladed impeller and ribbon impeller, were employed to establish the high-solid anaerobic digesters for the energy generation from WAS. The detailed flow patterns of two digesters were visualized by performing three-dimension CFD simulations. The mixing efficiency of two impellers was investigated by conducting tracing experiments and the high-solid WAS anaerobic digestion performance with two impellers were systematically explored. Moreover, the surplus energy was also evaluated. This work has delivered a comprehensive comparison of two typical impellers and has revealed the reason for the efficiency differences through experimental effects, mixing characteristics and mixing modes, which might have benefited the design and operation of anaerobic digestion systems.

2. Materials and methods

2.1. Configuration of high-solid sludge anaerobic digester

A custom-built horizontal anaerobic digester manufactured with stainless steel was employed in this work, as shown in Fig. 1. It had an empty volume of 200 L with an inner diameter of 500 mm, a height of 600 mm and a length of 750 mm, and provided a working volume of 160 L. Two types of impellers, viz. double-bladed impeller and ribbon impeller, were equipped in the digester successively. Both the two impellers were commissioned with stainless steel and the detail structure parameters were summarized in Supporting information (SI), Table S1. The digestion temperature was maintained at 35 ± 2 °C by a water bath jacket with an electric heating system. A digital sensing torque meter (GB-DTS500/GB-ZNM, Gongbiao, China) was connected to the rotation axis to acquire torque data.

2.2. Computational fluid dynamic simulation

The entity models of anaerobic digesters equipped with the double-bladed impeller and ribbon impeller were established by SolidWorks software (version 2015, SolidWorks, USA). Mesh dividing process was conducted by a pretreatment software named Gambit (2.4.6, Fluent Inc., USA), as illustrated in SI, Fig. S1. Given the irregular shape of the digester with impeller, the unstructured mesh dividing method was adopted. The effect of mesh size on the accuracy of CFD simulation was evaluated by the mesh independence test which has been presented in SI, Table S2. The simulated torque was selected to assess the mesh dividing schemes. The relative error between adjacent meshing schemes continuously decreased by refining mesh size. In this work, the relative error below 2% was considered as the criteria to choose the appropriate mesh dividing scheme.

A three-dimensional CFD simulation was used to investigate the hydrodynamics of the digesters with the double-bladed impeller and ribbon impeller through commercially available CFD software ANSYS Fluent (15.0, ANSYS Inc., USA). Tecplot (Tecplot 360, USA) was used for post-processing. A 64-bit workstation with Intel® Core ™ i7-7700 K @ 4.20 GHz processor and 16 GB of RAM was used for computational work. Due to the complexity of the actual digester and the anticipation for obtaining accuracy of the simulation process, several hypotheses and simplifications are portrayed drawn as in SI.

The WAS was considered as one single homogeneous phase and acted as non-Newtonian fluid (Wu, 2012). The Herschel-Bulkley model was adopted to describe the rheological behavior of WAS in the present work:

$$\tau = \tau_0 + k\gamma^n \tag{1}$$

where τ is the shear stress, Pa; τ_0 is the yield stress, Pa; γ is the shear rate, 1/s; k is the consistency coefficient, Pa·s^n; n is the power low index. These indexes were quantified by WAS rheology using a rotational rheometer (Advanced Rheometer Physica MCR301, Anton Paar Inc, Austria). WAS with total solids (TS) of 12.25% was adopted for rheology experiments at a temperature of 35 ± 2 °C. The shear rate was controlled from 0.01 to 1000 s^{-1} and the duration time was 8 s as shown in Fig. S2. In the present work, the density of WAS was 1071 kg/m^3, the τ_0, k and n were calculated as 137.41 Pa, 15.34 Pa·s^n and 0.42, respectively. Based on the theoretical calculation and previous researches (Terashima et al., 2009; Wu, 2012), the laminar flow model was used to investigate the hydrodynamics.

In order to minimize the computational complexity and increase the computational stability, the simulated regions were divided into fluid-rotation region and fluid-station region using multiple reference frames method (MRF). No-slip boundary conditions were applied on the wall. A "steady-state" solver was chosen to visualize the flow pattern of digesters equipped with double-bladed impeller and ribbon impeller. The SIMPLE algorithm was used to solve velocity–pressure coupling, 2nd UPWIND numerical scheme was used for discretization of momentum, and other parameters were maintained as the default values. Relative tolerance of accuracy of the CFD simulations was the convergence criterion below 10^{-6}.

2.3. Mixing time model

In order to assess the mixing efficiency of the digesters with double-bladed and ribbon impellers, the mixed time determination was carried out by tracing experiment. A total of 16,000 beads, made of plexiglass (desity of 1180 kg/m^3) and nonreactive and insoluble, with a diameter of 4 mm were employed as tracers and added in the digesters that loaded with working volume of
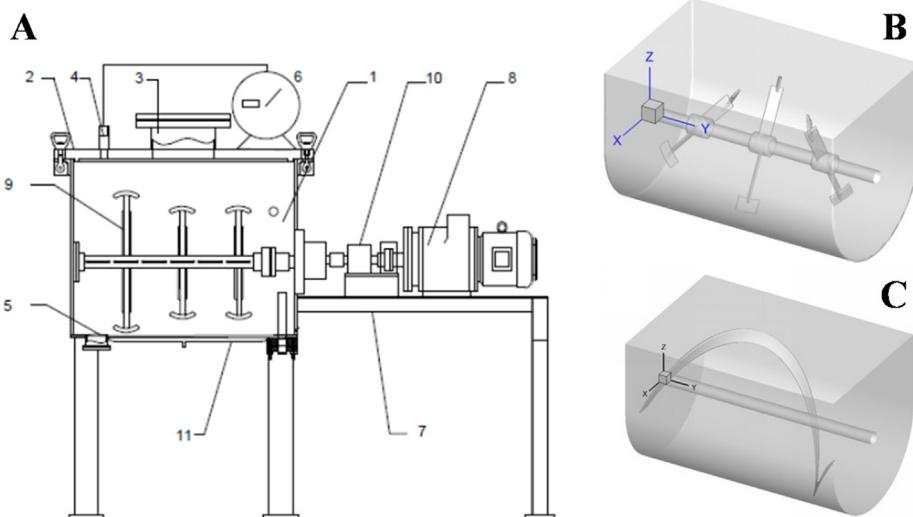
Fig. 1. Schematic diagram of the horizontal high-solid anaerobic digester (A) and the entity models of anaerobic digesters equipped with the double-bladed impeller (B) and ribbon impeller (C). (1) Digestion tank, (2) Cover plate, (3) Inlet, (4) Gas outlet, (5) Outlet, (6) Gas flow meter, (7) Holder, (8) Motor, (9) Impeller, (10) Digital sensing torque meter, (11) Water bath jacket.

WAS. The extra volume increment caused by adding tracers was negligible due to the beads volume was less than 0.4% of the working volume of the entire digester. The sludge samples with tracers were collected from the outlet at set intervals to count the beads. The beads were separated from sludge using a screen with mesh size of 3 mm. The degree of homogeneity was calculated as follows:

$$M(t) = \frac{|c_i(t) - c_{ave}|}{c_{ave}} \times 100\% \tag{2}$$

where $M(t)$ is the degree of homogeneity; $Ci(t)$ is the tracer concentration, pcs/L; C_{ave} is the average tracer concentration based on the theoretical calculation, which is 100 pcs/L. Mixing time (t_{80}), is defined as that required to achieve $M(t) \leq 20\%$, s.

2.4. High-solid WAS anaerobic digestion experiment

High-solid WAS anaerobic digestion experiment was conducted to evaluate the influence of the impeller type on the digestion performance and energy efficiency. The feedstock WAS was collected from a local wastewater treatment in Wuxi, China, in which an A^2/O process was operated with a capability of 40,000 t/d (equivalent to 200,000 inhabitants). The thick WAS was dewatered by a belt filter press and the dewatered WAS was collected by plastic bags. The TS, volatile solids (VS), VS/TS, pH, ammonium nitrogen and alkalinity were 12.98 ± 0.52%, 6.94 ± 0.28%, 53.46 ± 1.75%, 7.29 ± 0.01, 459.09 ± 10.02 mg/L and 585.13 ± 11.60 mg-CaCO₃/L, respectively.

The inoculum was collected from a WAS anaerobic digestion reactor with a volume of 50 m³. It was operated in a semi-continuous mode for more than one year with a sludge retention time of 35 days. The main characteristics of inoculum were as follows: TS of 12.06 ± 0.05%, VS of 5.08 ± 0.11%, VS/TS of 42.12 ± 0.05%, pH of 8.94 ± 0.01, ammonium nitrogen of 4391.42 ± 9.74 mg/L and alkalinity of 9041.03 ± 13.50 mg-CaCO₃/L, respectively.

The start-up of the horizontal anaerobic digester was conducted with the double-bladed impeller and the TS ratio of inoculum and WAS was 15:85. Part of the digested sludge was replaced by fresh WAS every 4 days to maintain a sludge retention time of 30 days. The start-up stage lasted for two months and the data of the start-

up stage has been described in our previous publication (Yang et al., 2018).

The digestion experiment was divided into six stages as displayed in Table 1. In stage I-III, the horizontal digester was equipped with the double-bladed impeller and operated at 10, 25 and 50 rpm, respectively. The double-bladed impeller was replaced by ribbon impeller at the end of stage III. In stage IV-VI, the horizontal digester was equipped with the ribbon impeller and operated at 10, 25 and 50 rpm, respectively. The WAS anaerobic digestion experiment was conducted in a semi-continuous mode with a sludge retention time of 30 days, about 1/15 of the digested sludge was replaced by fresh WAS every two days. The experimental results of each stage were presented with "mean values ± standard deviations".

2.5. Analytical and calculational methods

The sludge samples were collected from the digester once in two days and centrifuged at 8000 rpm for 10 min by a centrifuge (AG 22331, Eppendorf, Germany). The supernatant was immediately filtered through 0.45 μm filters (Tianjin Jinteng Experiment Equipment Co., Ltd., China). The TS, VS, ammonium nitrogen and alkalinity were quantified according to standard methods (EPA, 2002). The pH was measured by an acidity meter (FE28, Mettler Toledo, China). The free ammonia concentration was calculated according to the previous literature with the following equation (Duan et al., 2012):

$$\frac{[NH_3]}{[AN]} = \left[1 + \frac{10^{-pH}}{10^{-\left(0.09018 + \frac{2729.92}{T}\right)}} \right]^{-1} \tag{3}$$

where the $[NH_3]$ is the concentration of ammonium nitrogen, mg/L; $[AN]$ is the concentration of free ammonia, mg/L; T is the thermodynamic temperature, K.

Biogas production was quantified by a wet gas flow meter (LMF-2, Beijing Jinzhiye Instrument equipment Co. LTD, China) and the content (including methane and carbon dioxide) was analyzed by a gas chromatograph (GC9790II, FuLi, China) equipped with a stainless-steel column (AE. TDX-01, Φ3mm × 2 m, China). The injection temperature was 150 °C and Ar (99.99%) was used as carrier gas. The oven temperature was maintained at 80 °C

Table 1
The design of the high-solid WAS anaerobic digestion experiment.

Stage	I	II	III	IV	V	VI
Operational period (d)	32	30	32	39	40	40
Agitation time (h/d)	6	6	6	1	0.38	0.16
Rotational speed (rpm)	10	25	50	10	25	50
Impeller type	Double-bladed impeller			Ribbon impeller		

and the samples were analyzed with a thermal conductivity detector at 150 °C and the detect electricity was 80 mA.

The agitation power was calculated by the torque value from the motor, which is acquired in a digital sensing torque meter:

$$P = \frac{2\pi NT}{60} \tag{4}$$

where P is power consumption, W; T is toque, N·m.

The agitation energy consumption (Ea, J) was defined as follow:

$$Ea = \frac{Pt}{1000} \times 3.6 \times 10^6 \tag{5}$$

where t is agitation time, h.

The energy generation was evaluated by methane production and calorific value (E, J):

$$E = Q\omega \times 3.59 \times 10^7 \tag{6}$$

where the Q is biogas production, m^3; ω is the methane proportion in biogas, %; 3.59×10^7 is the methane calorific value, J/m^3.

The surplus energy was calculated as follow:

$$\text{Surplus energy} = \frac{E - Ea}{V \cdot \frac{t}{24}} \tag{7}$$

where the V is the effect volume of digester, m^3.

3. Results and discussion

3.1. Flow pattern visualization of digesters with double-bladed and ribbon impeller

CFD simulations were employed to depict the hydrodynamic characteristics of the digesters that were successively equipped with double-bladed impeller and ribbon impeller, and the visual representations were derived. After 9898, 10,514 and 11,351 iterations, the residuals of double-bladed impeller simulations at 10, 25 and 50 rpm were converged to 10^{-6}, and 7056, 9453 and 12,162 iterations for ribbon impeller, as displayed in Fig. S3. Three representative profiles, X = 0, Y = 375 and Z = 0 mm (referred to Fig. S1), were extracted to assess the hydrodynamics characteristics. The agitation was driven by the axis and transferred to the fluid (WAS) by the impeller, thus higher rotation speed brought higher fluid velocity as presented in Fig. 2. For the double-bladed impeller, the velocity was increased along the paddle and reached the maximum at the end of the paddle. By invigorating rotation speed, the velocity of the central part of the fluid field was amplified, yet the near-wall region was almost impervious. The conditions in the ribbon impeller were different as high-velocity region was distributed around the blade. The near-axis region remained low velocity even at a rotation speed of 50 rpm.

The diverse configurations of the double-bladed impeller and ribbon impeller resulted in divergent mixing efficiencies. The blades of double-bladed impeller were perpendicular to the axis of rotation, and driving force was derived from the center and developed towards the wall of the digester. Whereas, the ribbon impeller was installed along the wall and the driving force spread towards the rotation axis. This difference could be visually identified from Fig. 3, in which, the colored fluid region was encircled by

the contour with a velocity greater than 0.01 m/s. The high-velocity region prevailed forcefully around the paddle in both double-bladed impeller and ribbon impeller at 10 rpm. The colored region volume increased with the rotation speed that elevated to 25 and 50 rpm. It was obvious that the velocity over 0.01 m/s region in double-bladed impeller stayed at the center of the digester, the marginal area persisted a low velocity and potentially turned into a dead zone. The ribbon impeller provided a larger volume of active region compared to the double-bladed impeller, especially in the marginal area. The efficient utilization of the digester volume was indubitably benefited for the performance improvement (Cui et al., 2020). In addition to the mixing form, the mixing efficiencies of two types of impellers were discrepant. The ribbon impeller manifested an efficient mixing performance and given volume-average velocities of 0.017, 0.032 and 0.061 m/s at rotation speeds of 10, 25 and 50 rpm, respectively, which were 1.8, 2.0 and 2.2 times versus double-bladed impeller. Higher volume-average velocity indicated intensive mixing which optimistically influenced the sufficient interaction between the substrate and functional microbes, as well as the biogas emission (Sajjadi et al., 2016).

High-solid WAS was a non-Newtonian fluid and the rheological properties change was related to the agitation power consumption and anaerobic digestion performance (Liu et al., 2019b). The WAS viscosity variation was shown in Fig. 4, in general, the viscosity contours were quite similar to the velocity contours. The WAS viscosity showed a negative correlation with the distance to the paddle. The sludge in a quiescent state acquired the disorderly movement, and macromolecules were impeded to flow. When the shear stress was exerted on the sludge, macromolecules were warped and stretched. With the increase of shear stress, the molecular movement in the sludge was constantly increased and the viscosity was correspondingly reduced (Larson et al., 1999). The higher rotational speed resulted in higher shear stress. The sludge fluidity was enhanced with the increase of rotational speed, and the substrates homogeneity was achieved more effortlessly in the digester. By comparing to the double-bladed impeller, digester with the ribbon impeller emerged with a lower viscosity at the same rotation speed, indicating preferable fluidity and uniform mixing performance (Markis et al., 2016).

3.2. Mixing efficiency comparison of the double-bladed and ribbon impellers

The tracing experiment was conducted to explore the mixing efficiencies of digesters with double-bladed and ribbon impellers. The curves of tracer concentration versus mixing time were finally stabilized around 100 pcs/L which were near to the theoretical value (Fig. 5), indicating the relative thorough mixing could be achieved with both type impellers under all rotation speed conditions. However, the equilibrium values were approached by quite different modes with two impellers. The tracer concentrations of double-bladed impeller gradually ascended to terminal value, while the ribbon impeller fluctuated in a wide range and rapidly narrowed to the equilibrium value. The tracer was input on the surface of the sludge and the outlet was also located at the surface. The ribbon impeller initiated the mixing from the surface of the
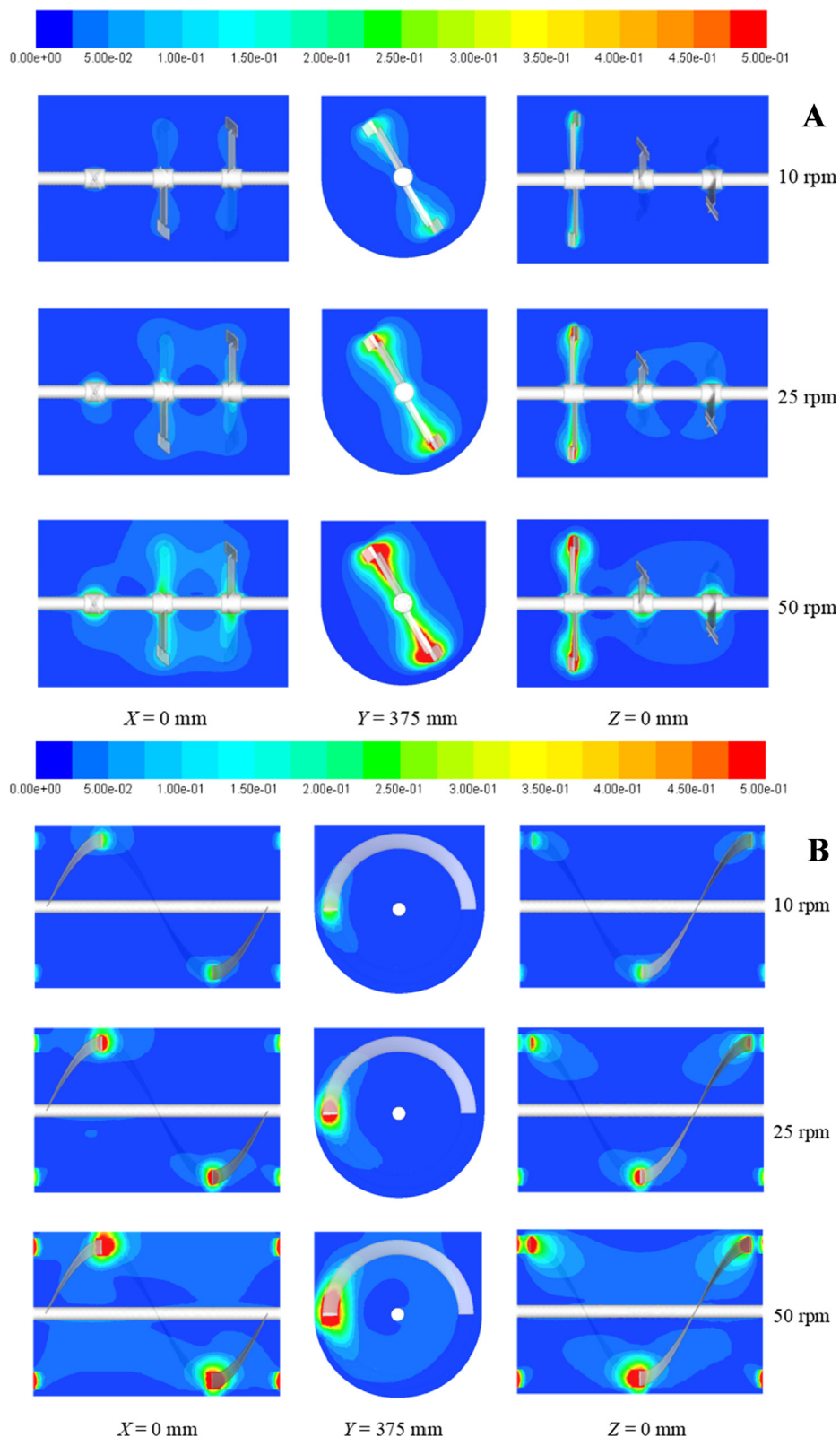
Fig. 2. Contours of velocity at rotating speeds of 10, 25 and 50 rpm. A, Double-bladed impeller; B, Ribbon impeller.

digester (see Fig. 3), the tracers motioned around the digester wall and passed the outlet repetitively then got completely mixed with the sludge. For the double-bladed impeller, the well-mixed zone was adjoining the impeller and the surface tracers were driven tardily. It could be concluded that the mixing of double-bladed impeller started from the center and advanced to the surface. On the contrary, the ribbon impeller was along the radial direction and progressed towards the axis.

The mixing time was distinctly different for the two impellers. The ribbon impeller was more efficient compared to double-
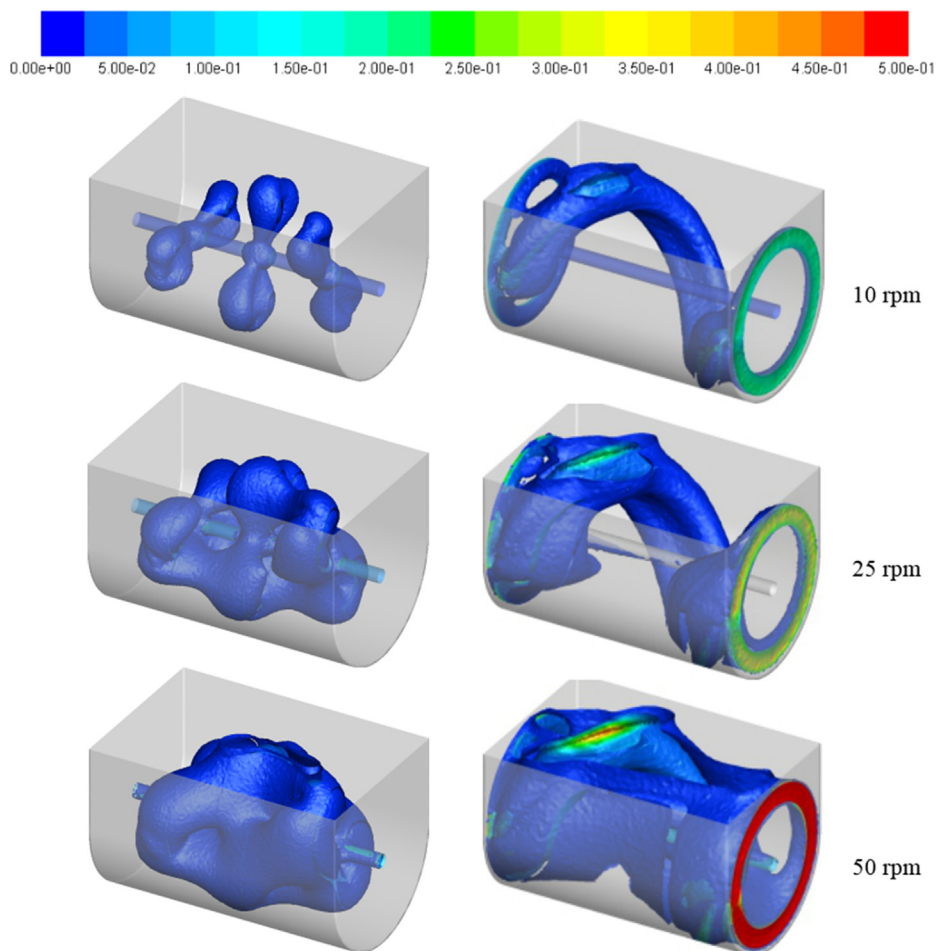
Fig. 3. Visual representation of region with velocity over 0.01 m/s at rotating speeds of 10, 25 and 50 rpm. Left, Double-bladed impeller; right, Ribbon impeller.

bladed impeller and the t_{80} was about 60 mins at 10 rpm and obviously decreased to 20 mins at 50 rpm. For the double-bladed impeller, homogeneous mixing consumed 360 mins at 50 rpm and further increased to 640 mins at 10 rpm (Table S3). The t_{80} of the digester with double-bladed impeller was about 10.7 to 18 times of the ribbon impeller at the same rotation speed conditions. It was also confirmed by the visual path lines produced by CFD in Fig. S4. For the double-bladed impeller digester, the particle trails were mainly near the impeller zone and few of path lines along the axis. While the path lines well-distributed in the entire digester with ribbon impeller indicated efficient mixing efficiency.

3.3. Anaerobic digestion performance of double-bladed and ribbon impeller

A 213-day long-term anaerobic digestion experiment was conducted to assess the influence of impeller type. According to Fig. 6, the digester with ribbon impeller presented preferable performance compared to double-bladed impeller. For the double-bladed impeller digester, the VS degradation rate was elevated from 12.46 ± 2.57% to 20.37 ± 3.45% with the rotation speed increased from 10 to 50 rpm. The biogas analysis indicated that methane and carbon dioxide were the major components with methane gas as the predominant one. The methane content was sustained at ~ 60% in the biogas and ~ 30% of carbon dioxide was identified at all conditions. The biogas yield increased from 104.0 9 ± 6.32 to 188.29 ± 23.28 mL/g VS and the corresponding methane yield of 56.60 ± 5.51 to 116.33 ± 16.65 mL/g VS. The ribbon

impeller attained a 27.97 ± 1.55% of VS degradation at 10 rpm and improved to 31.29 ± 1.33% at 50 rpm, the maximum biogas yield achieved 340.38 ± 15.91 mL/g VS (210.34 ± 7.55 mL-CH_4/g VS) which was about 1.8 times higher than double-bladed impeller. The biogas/methane yield from this study was reasonable compared to the previous works (as shown in SI, Table S4). Xu et al. (Xu et al., 2020) indicated that typical anaerobic digestion with WAS presented a VS degradation rate less than 35% and a methane yield less than 240 mL-CH_4/g VS.

During the anaerobic digestion of WAS, organic nitrogen was converted to inorganic nitrogen by hydrolysis, resulting in an increase in the ammonium concentration. The variation trend of ammonium concentration was similar to the VS degradation rate. In general, the digester with ribbon impeller accumulated more ammonium nitrogen and higher rotation speed was inclined to intensify the WAS degradation. The maximum ammonium concentration was recorded as 2110.11 ± 165.59 mg/L at 50 rpm with ribbon impeller. Ammonium nitrogen had no significant impact on the anaerobic digestion process, while it could be transformed to free ammonia with pH upsurge. pH was the key factor for the revelation of anaerobic digestion status and it also influenced the dynamic equilibrium between ammonium and free ammonia. The methanogens survived under the neutral conditions and methanogenesis consumed the organic acid resulting in a continuous pH upsurge (Liu et al., 2008). It was perceived that the highest pH was 8.04 ± 0.06 with ribbon impeller at 50 rpm, and provided a maximum free ammonia accumulation of 233.65 ± 40.82 mg/L. Free ammonia was reported to pose an inhibition on the anaerobes,
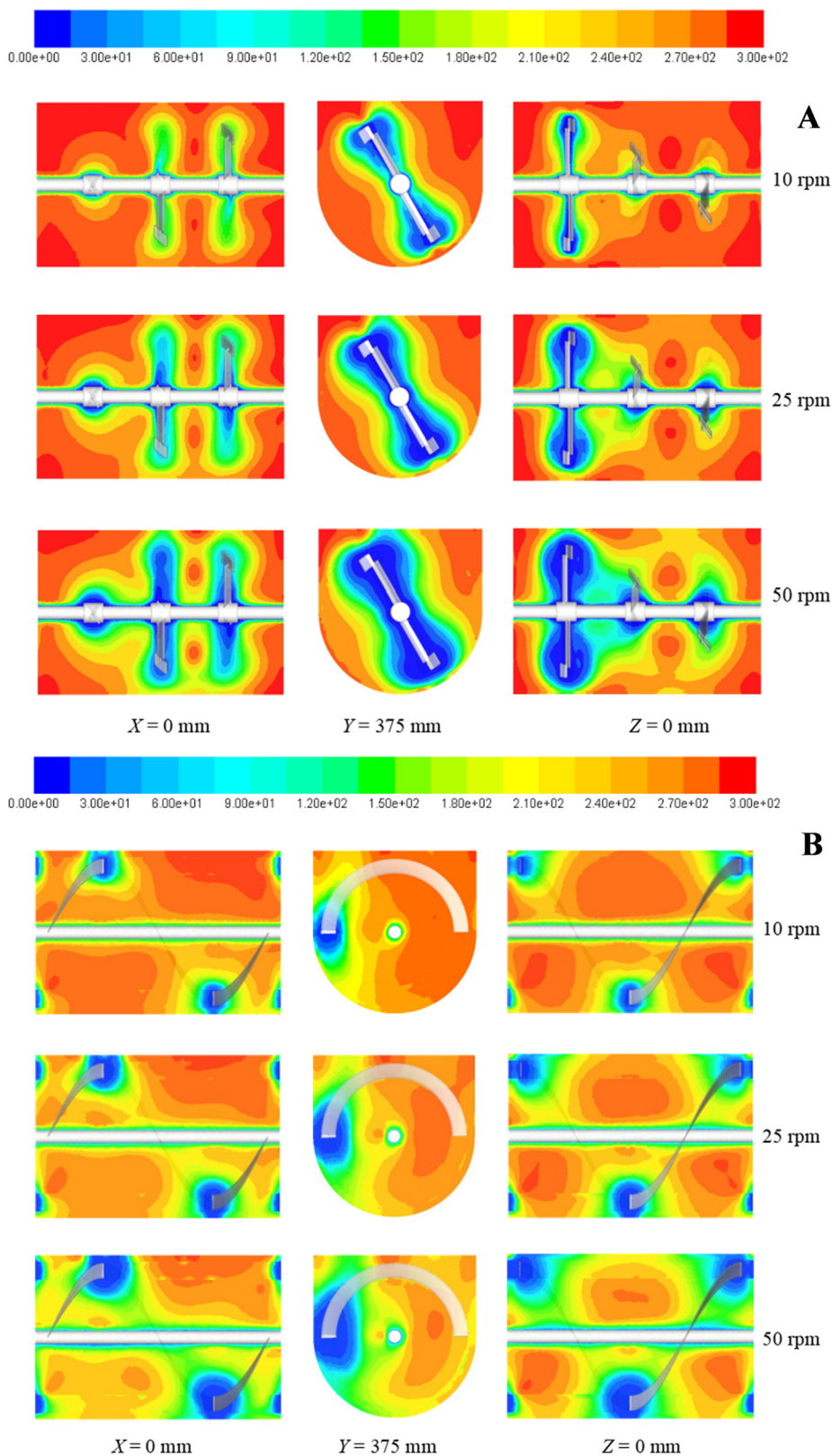
Fig. 4. Contours of apparent viscosity at rotating speeds of 10, 25 and 50 rpm. A, Double-bladed impeller; B, Ribbon impeller.

especially on the methanogens when the concentration was higher than 600 mg/L (Duan et al., 2012). Free ammonia concentrations in this work (<250 mg/L) were far lower than the inhibition threshold, implied the potential inhibition was slight. The alkalinity was reported in a range of 4099.25 ± 178.01 to 6010.67 ± 245.80 mg-CaCO$_3$/L in the digester with double-bladed impeller and 4780.66 ± 381.22 to 7530.59 ± 339.16 mg-CaCO$_3$/L with ribbon impeller, indicating the steady operation of WAS anaerobic digestion.
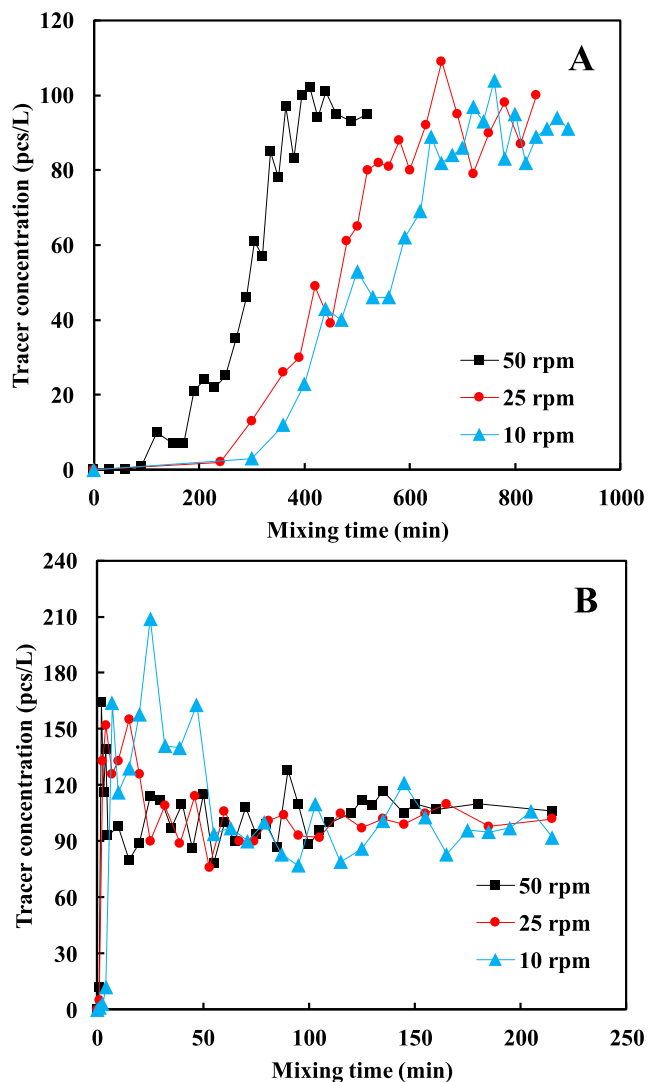
Fig. 5. Comparison of the mixing efficiencies of the double-bladed impeller (A) and ribbon impeller (B).

3.4. Energy analysis

The energy consumptions of double-bladed impeller and ribbon impeller at rotation speeds varying from 2 to 60 rpm were depicted in Fig. 7A. The agitation power was linearly increased with elevated rotation speed for both impellers. Ribbon impeller required higher torque and more energy consumption compared to double-bladed impeller. It was recorded as 11.31, 29.71 and 70.69 W at 10, 25 and 50 rpm for ribbon impeller, which were about 1.3, 1.3 and 1.5 times of that with double-bladed impeller at the corresponding conditions, respectively.

Considering the account of energy recovery from biogas, anaerobic digestion of WAS presented positive energy benefits at all conditions as revealed in Fig. 7B. The maximum surplus energy of double-bladed impeller digester was recorded as 4.53 ± 0.52 MJ/($m^3 \cdot d$) at a rotation speed of 50 rpm for an agitation time of 6 h/d which was about one mixing time (t_{80}). Reducing the agitation time obviously decreased the agitation energy consumption, however, the surplus energy was debilitated due to the deterioration of anaerobic digestion performance. The ribbon impeller digester merely disbursed 0.25 MJ/($m^3 \cdot d$) to achieve a t_{80} of 60 min at 10 rpm and provided surplus energy of 11.55 ± 2.00 MJ/($m^3 \cdot d$). By the reduction of the agitation time and intensification of the rotation speed to maintain the agitation energy at 0.25 MJ/($m^3 \cdot d$), surplus energy was gradually lifted to 16.23 ± 0.76 MJ/($m^3 \cdot d$).

These findings demonstrated that the anaerobic digestion with ribbon impeller was much more advantageous than the double-bladed impeller in terms of energy efficiency. The double-bladed digester required higher energy consumption to acquire efficient mixing and thereby facilitate methane production. Agitation energy consumption of ribbon impeller was only 5.2% to 22.6% of that in double-bladed impeller and the surplus energy was about 2 times higher at the equivalent rotation speed.

Although the ribbon impeller required higher initial power, it achieved well-mixed status in quite short time and remarkably enhanced the biogas production. Thus, the energy efficiency of ribbon impeller was obviously superior to double-bladed impeller. However, more attention should be paid on the mechanical strength and toughness of the ribbon impeller material in terms of practical application, especially with the intermittent mixing
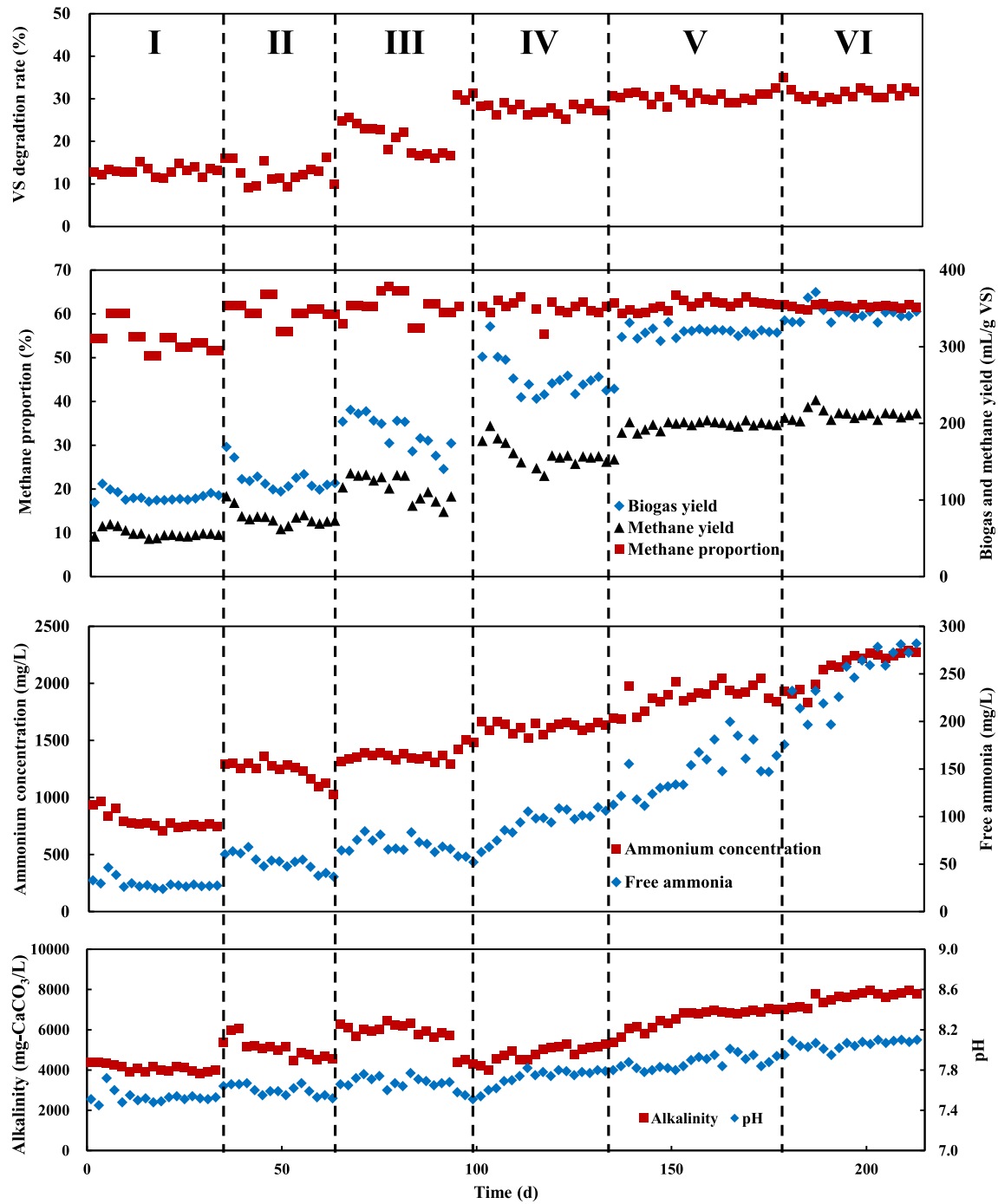
Fig. 6. Anaerobic digestion performance at various conditions. Stage I, II and III represent the digester with double-bladed impeller at rotation speeds of 10, 25 and 50 rpm, respectively; Stage IV, V and VI represent the digester with ribbon impeller at rotation speeds of 10, 25 and 50 rpm, respectively.
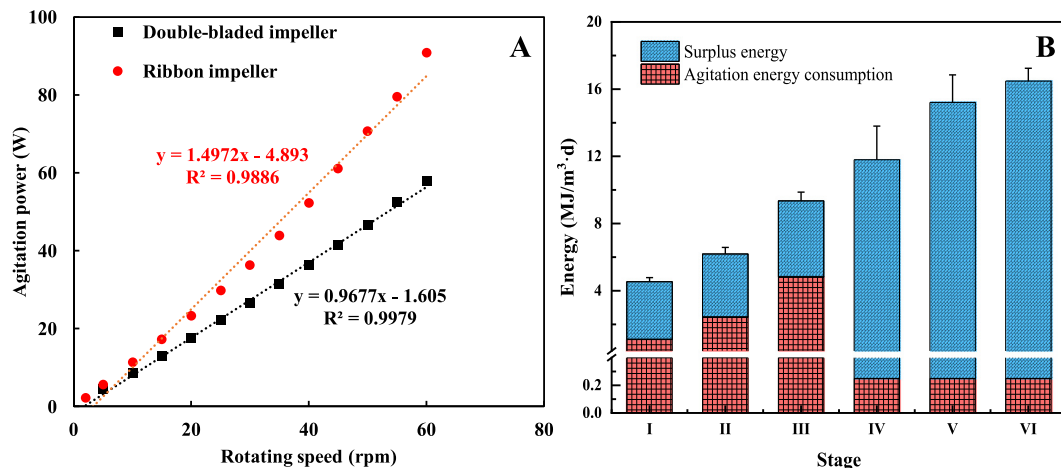
Fig. 7. Comparison of the rotation power of double-bladed impeller and ribbon impeller (A) and energy analysis of the digester equipped with double-bladed impeller and ribbon impeller (B). Stage I, II and III represent the digester with the double-bladed impeller at rotation speeds of 10, 25 and 50 rpm, respectively; Stage IV, V and VI represent the digester with ribbon impeller at rotation speeds of 10, 25 and 50 rpm, respectively.

mode. Besides, the spatial configuration of ribbon impeller used in the full scale WAS digester needs to be carefully designed.

4. Conclusions

In this work, the consequences of the double-bladed impeller and ribbon impeller on WAS anaerobic digestion were ascertained. Ribbon impeller was preferable to provide efficient mixing performance with lower energy consumption and higher net biogas production than the double-bladed impeller, and contributed to a superior surplus energy output. The CFD simulation of velocity and apparent viscosity distribution visually revealed that the various mixing modes were the responsible for the variations. This study thus provided a comprehensive and in-depth understanding of the effects of impeller construction and mixing strategies on the high-solid anaerobic digestion of WAS, which were benefited the design and operation of anaerobic digestion systems.

Declaration of Competing Interest

The authors declare that they have no known competing financial interests or personal relationships that could have appeared to influence the work reported in this paper.

Appendix A. Supplementary material

Supplementary data to this article can be found online at https://doi.org/10.1016/j.wasman.2020.11.054.

References

Cui, M.-H., Sangeetha, T., Gao, L., Wang, A.-J., 2020. Hydrodynamics of up-flow hybrid anaerobic digestion reactors with built-in bioelectrochemical system. J. Hazard Mater., 382

Dapelo, D., Bridgeman, J., 2018. Assessment of mixing quality in full-scale, biogas-mixed anaerobic digestion using CFD. Bioresour. Technol. 265, 480–489.

Duan, N., Dong, B., Wu, B., Dai, X., 2012. High-solid anaerobic digestion of sewage sludge under mesophilic conditions: Feasibility study. Bioresour. Technol. 104, 150–156.

EPA, C., 2002. Water and wastewater monitoring and analysis method

Kowalczyk, A., Harnisch, E., Schwede, S., Gerber, M., Span, R., 2013. Different mixing modes for biogas plants using energy crops. Appl. Energy 112, 465–472.

Larson, R.G, Vermant, Kröger, 1999. The structure and rheology of complex fluids.

Liu, D., Zeng, R.J., Angelidaki, I., 2008. Effects of pH and hydraulic retention time on hydrogen production versus methanogenesis during anaerobic fermentation of organic household solid waste under extreme-thermophilic temperature (70 degrees C). Biotechnol. Bioeng. 100, 1108–1114.

Liu, X., Yuan, W., Di, M., Li, Z., Wang, J., 2019a. Transfer and fate of microplastics during the conventional activated sludge process in one wastewater treatment plant of China. Chem. Eng. J. 362, 176–182.

Liu, Y., Chen, J., Song, J., Hai, Z., Lu, X., Ji, X., Wang, C., 2019b. Adjusting the rheological properties of corn-straw slurry to reduce the agitation power consumption in anaerobic digestion. Bioresour. Technol. 272, 360–369.

Mahmoodi-Eshkaftaki, M., Ebrahimi, R., 2019. The effect of blade angle of turbine impellers on anaerobic digestion efficiency in stirred digesters. Energy 178, 772–780.

Markis, F., Baudez, J.C., Parthasarathy, R., Slatter, P., Eshtiaghi, N., 2016. Predicting the apparent viscosity and yield stress of mixtures of primary, secondary and anaerobically digested sewage sludge: Simulating anaerobic digesters. Water Res. 100, 568–579.

Pastor-Poquet, V., Papirio, S., Harmand, J., Steyer, J.P., Trably, E., Escudie, R., Esposito, G., 2019a. Assessing practical identifiability during calibration and cross-validation of a structured model for high-solids anaerobic digestion. Water Res. 164, 114932.

Pastor-Poquet, V., Papirio, S., Trably, E., Rintala, J., Escudié, R., Esposito, G., 2019b. High-solids anaerobic digestion requires a trade-off between total solids, inoculum-to-substrate ratio and ammonia inhibition. Int. J. Environ. Sci. Technol. 16, 7011–7024.

Sadino-Riquelme, C., Hayes, R.E., Jeison, D., Donoso-Bravo, A., 2018. Computational fluid dynamic (CFD) modelling in anaerobic digestion: General application and recent advances. Crit. Rev. Environ. Sci. Technol. 48, 39–76.

Sajjadi, B., Raman, A.A.A., Parthasarathy, R., 2016. Fluid dynamic analysis of non-Newtonian flow behavior of municipal sludge simulant in anaerobic digesters using submerged, recirculating jets. Chem. Eng. J. 298, 259–270.

Singh, B., Szamosi, Z., Siménfalvi, Z., 2019. State of the art on mixing in an anaerobic digester: A review. Renewable Energy 141, 922–936.

Terashima, M., Goel, R., Komatsu, K., Yasui, H., Takahashi, H., Li, Y.Y., Noike, T., 2009. CFD simulation of mixing in anaerobic digesters. Bioresour. Technol. 100, 2228–2233.

Wei, W., Wu, L., Liu, X., Chen, Z., Hao, Q., Wang, D., Liu, Y., Peng, L., Ni, B.-J., 2020. How does synthetic musks affect methane production from the anaerobic digestion of waste activated sludge?. Sci. Total Environ., 713

Wu, B., 2012. CFD simulation of mixing for high-solids anaerobic digestion. Biotechnol. Bioeng. 109, 2116–2126.

Xu, Y., Lu, Y., Zheng, L., Wang, Z., Dai, X., 2020. Perspective on enhancing the anaerobic digestion of waste activated sludge. J. Hazard. Mater. 389, 121847.

Yang, M., Zheng, Z., Yu, L., Zhang, L., Lu. Shuailing, Cui, M., Liu, H., Liu, H., 2018. Study on the characteristics of a horizontal anaerobic digestion reactor for treatment of high-solid sludge. Environ. Pollution & Control 40, 1224–1228.

Zhang, J., Mao, L., Nithya, K., Loh, K.-C., Dai, Y., He, Y., Wah Tong, Y., 2019. Optimizing mixing strategy to improve the performance of an anaerobic digestion waste-to-energy system for energy recovery from food waste. Appl. Energy 249, 28–36.